

Numerical solutions for unsteady flow past a semi-infinite inclined plate with temperature oscillations[†]

G.Palani and Kwang-Yong Kim*

Department of Mechanical Engineering, Inha University Incheon, 402-751, Korea

(Manuscript Received October 16, 2008; Revised March 18, 2009; Accepted March 23, 2009)

Abstract

A study of the velocity and thermal boundary layers on a semi-infinite inclined plate with temperature oscillations is presented in this work. The non-linear, coupled parabolic integro-partial differential equations governing flow and heat transfer have been solved numerically using an implicit finite difference scheme of Crank-Nicolson type. The numerical values for the flow field, temperature, shearing stress, and heat transfer coefficients are presented in a graphical form. It is observed that the velocity and temperature profiles decrease as the frequency parameter increases.

Keywords: Finite difference; Oscillations; Transient flow; Grashof number; Skin friction

1. Introduction

Natural convection heat transfer plays an important role in our environment and in many engineering devices. The buoyancy force induced by the density differences in a fluid causes natural convection. The applications include, for example, the cooling of the core of a nuclear reactor in the case of a pump, or power failures and the warming and cooling of electronic components. Fujii and Imura [1] studied experimentally the natural convection heat transfer from a plate with arbitrary inclination using two plates with different dimensions. Pera and Gebhart [2] studied the laminar natural convection boundary layer flow above horizontal and slightly inclined surfaces with uniform temperature and heat flux. Perturbation analysis was employed to solve the problem. Chen et al. [3] studied the flow and heat transfer characteristics of laminar free convection in boundary layer flows from horizontal, inclined, and vertical plates with variable wall temperature and heat flux. Ekam-

bavannan and Ganesan [4] presented a finite-difference solution of unsteady natural convection boundary layer flow over an inclined plate with variable surface temperature. These problems are of basic importance, thus other physical situations also need investigation. One such case is when the plate temperature is oscillating; how is the flow affected? Such issue is particularly important and useful in the fields of space science, nuclear engineering, structural engineering, and so on.

Keller and Yang [5] studied the heat transfer responses of a laminar free convection boundary layer along a vertical heated plate to surface temperature oscillations, when the mean surface temperature is proportional to x^{-n} , where x^{-n} is the distance measured from the leading edge of the plate. An exact analysis of Stoke's problem for an infinite vertical plate, whose temperature varies linearly with time, was studied by Soundalgekar and Patil [6]. The motion of a semi-infinite incompressible viscous fluid caused by the oscillations of a vertical plate was studied by Soundalgekar [7]. They derived closed-form solutions to velocity, temperature, and penetration distance through which the leading edge effect propagates. The two-dimensional unsteady flow of a viscous in-

[†] This paper was recommended for publication in revised form by Associate Editor Yang Na

* Corresponding author. Tel.: +82 32 860 7317, Fax.: +82 32 868 1716

E-mail address: kykim@inha.ac.kr

© KSME & Springer 2009

compressible fluid past an infinite vertical plate has been studied by Soundalgekar [8] under the following conditions: (i) constant suction at the plate, (ii) wall temperature oscillating at a constant non-zero mean, and (iii) a constant free stream. The approximate solutions to the coupled non-linear equations governing the flow have been carried out for transient velocity, transient temperature, the amplitude and phase of skin friction, and the rate of heat transfer. Verma [9] analyzed the effect of the oscillation of surface temperature on unsteady free convection from a horizontal plate. Soundalgekar et al. [10] studied the flow of a viscous incompressible fluid past an impulsively started infinite vertical plate in the presence of foreign mass under the condition of variable plate temperature and constant heat flux. Houssain [11] solved the problem of simultaneous heat and mass transfer in two-dimensional free convection from a semi-infinite vertical flat plate. An integral method is used to find a solution for zero wall velocity with small-amplitude oscillatory wall temperature. Das et al. [12] addressed the transient free convection flow past an infinite vertical plate with the periodic oscillation of surface temperature. They simplified the problem by assuming small values of the Grashof number Gr ($\ll 1$). In this case, the temperature is independent of the flow, and the heat is transferred by conduction only. They used the Laplace transform technique to solve the simplified equations, and the results show that the transient velocity profile and the penetration distance decrease with an increase in the frequency of plate temperature oscillation. Hossain et al. [13] studied the heat-transfer response of a laminar free convection boundary layer flow of a viscous incompressible and electrically conducting fluid along a vertical plate to surface temperature oscillations. Revankar [14] investigated the free convection effects on flow field for two cases: (1) when a submerged infinite plate is set into motion impulsively with oscillating plate temperature, and (2) when the submerged infinite plate is set into motion with linear harmonic oscillation parallel to itself with oscillating temperature. The exact solutions for temperature and flow field are presented. The steady and unsteady free convection from a vertical wall with stream-wise surface temperature oscillation was investigated by Li et al. [15]. For small values of the Grashof number, they obtained an asymptotic formula for the average Nusselt number using a perturbation method. Lorenzo and Padet [16] conducted a parametric study of the free convection

along the vertical wall when a periodic heat flux density containing adiabatic period is applied. Their results show the importance of the adiabatic period to let the surrounding fluid refresh itself before applying a new heating period, leading to an increase in free convection heat transfer. Rani and Devaraj [17] presented a numerical solution for free convection flow past a vertical cylinder with temperature oscillations. They solved non-dimensional governing equations by using an implicit finite difference scheme of Crank-Nicolson type. The effect of the periodic oscillation of the surface temperature on the transient free convection from a vertical plate was investigated by Saeid [18]. They observed that increasing the amplitude and the frequency of the oscillating surface temperature will decrease the free convection heat transfer from the plate to both air and water.

The unsteady natural convection flow past a semi-infinite inclined plate with temperature oscillations has been given very scant attention in the literature. Hence, we propose to study the problem of heat transfer effects on a semi-infinite inclined plate with temperature oscillations. The governing boundary layer equations are first cast into a dimensionless form, and the resulting system of equations is then solved by an implicit finite difference scheme. In the present analysis, a relatively higher Grashof number is considered ($10^4 < Gr < 10^9$), where the laminar boundary layer is applicable for studying the effect of oscillating plate temperature on the free convection effects on the semi-infinite inclined plate.

2. Mathematical analysis

We consider a two-dimensional unsteady flow of a viscous incompressible fluid flow past a semi-infinite inclined plate with temperature oscillations. The analysis of the present paper is based on the following assumptions:

- (1) The plate makes an inclination angle ϕ to the horizontal.
- (2) The x -axis is measured along the plate, and the y -axis is taken along upward normal to the plate.
- (3) Initially at time $t' \leq 0$, it is assumed that the plate and the fluid are at the same temperature, and at time $t' > 0$, the temperature of the plate is maintained at an oscillating temperature.
- (4) The effect of viscous dissipation is not considered in the energy equation.
- (5) All the fluid properties are assumed to be con-

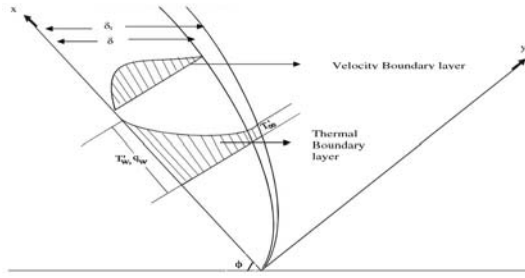


Fig. 1. Schematic diagram.

stant, except for the influence of density variation with temperature, which is considered only in the body force term.

(6) There is no chemical reaction between the diffusing species and the fluid.

By assuming Boussinesq's approximation, the unsteady two-dimensional boundary layer flow can be shown to be governed by the following equations:

$$\frac{\partial u}{\partial x} + \frac{\partial v}{\partial y} = 0 \tag{1}$$

$$\frac{\partial u}{\partial t'} + u \frac{\partial u}{\partial x} + v \frac{\partial u}{\partial y} = g \beta \cos \phi \frac{\partial}{\partial x} \int_0^\infty (T' - T'_\infty) dy + g \beta \sin \phi (T' - T'_\infty) + v \frac{\partial^2 u}{\partial y^2} \tag{2}$$

$$\frac{\partial T'}{\partial t'} + u \frac{\partial T'}{\partial x} + v \frac{\partial T'}{\partial y} = \alpha \frac{\partial^2 T'}{\partial y^2} \tag{3}$$

The initial and boundary conditions are as follows:

$$\begin{aligned} t' \leq 0 : u = 0, \quad v = 0, \quad T' = T'_\infty, \\ t' > 0 : u = 0, \quad v = 0, \quad T' \\ &= (T'_w - T'_\infty) \cos \omega t' + T'_w \quad \text{at } y = 0 \\ u = 0, \quad T' = T'_\infty, \quad &\text{at } x = 0 \\ u \rightarrow 0, \quad T' \rightarrow T'_\infty, \quad &\text{as } y \rightarrow \infty \end{aligned} \tag{4}$$

where \bar{u} and \bar{v} are the velocity components in the x and y directions, respectively; α is the thermal diffusivity; g is the acceleration due to gravity; t' is the time; T' is the temperature of the fluid in the boundary layer; β is the volumetric coefficient of thermal expansion; ν is the kinematic viscosity; ω is the frequency parameter; and ϕ is the inclination angle to the horizontal.

The following non-dimensional quantities are introduced:

$$\begin{aligned} X = \frac{x}{L}, \quad Y = \frac{y}{L} Gr^{1/4}, \quad U = \frac{uL}{\nu} Gr^{-1/2}, \\ V = \frac{vL}{\nu} Gr^{-1/4}, \quad t = \frac{\nu t'}{L^2} Gr^{1/2}, \quad T = \frac{T' - T'_\infty}{T'_w - T'_\infty} \\ Gr = \frac{g \beta L^3 (T'_w - T'_\infty)}{\nu^2}, \\ \omega = \frac{L^2 \omega'}{\nu} Gr^{-1/2} \quad Pr = \frac{\nu}{\alpha} \end{aligned} \tag{5}$$

Eqs. (1)-(4) are reduced to the following non-dimensional form:

$$\frac{\partial U}{\partial X} + \frac{\partial V}{\partial Y} = 0 \tag{6}$$

$$\begin{aligned} \frac{\partial U}{\partial t} + U \frac{\partial U}{\partial X} + V \frac{\partial U}{\partial Y} \\ = Gr^{-1/4} \cos \phi \frac{\partial}{\partial X} \int_0^\infty T dY + T \sin \phi + \frac{\partial^2 U}{\partial Y^2} \end{aligned} \tag{7}$$

$$\frac{\partial T}{\partial t} + U \frac{\partial T}{\partial X} + V \frac{\partial T}{\partial Y} = \frac{1}{Pr} \frac{\partial^2 T}{\partial Y^2} \tag{8}$$

The corresponding initial and boundary conditions in dimensionless form are as follows:

$$\begin{aligned} t \leq 0 : U = 0, \quad V = 0, \quad T = 0, \\ t > 0 : U = 0, \quad V = 0, \quad T = 1 + \cos \omega t, \quad \text{at } Y = 0 \\ U = 0, \quad T = 0, \quad &\text{at } X = 0 \\ U \rightarrow 0, \quad T \rightarrow 0, \quad &\text{as } Y \rightarrow \infty \end{aligned} \tag{9}$$

The non-dimensional forms of local and average skin friction, Nusselt number, are as follows:

$$\tau_x = Gr^{3/4} \left(\frac{\partial U}{\partial Y} \right)_{Y=0} \tag{10}$$

$$\bar{\tau} = Gr^{3/4} \int_0^1 \left(\frac{\partial U}{\partial Y} \right)_{Y=0} dX \tag{11}$$

$$Nu_x = -X Gr^{1/4} \left(\frac{\partial T}{\partial Y} \right)_{Y=0} / T_{Y=0} \tag{12}$$

$$\bar{Nu} = -Gr^{1/4} \int_0^1 \left(\frac{\partial T}{\partial Y} \right)_{Y=0} / T_{Y=0} dX \tag{13}$$

3. Numerical techniques

The two-dimensional, non-linear, unsteady, coupled, and integro-partial differential Eqs. (6)-(8) under

the initial and boundary conditions (9) are solved by using an implicit finite difference scheme of the Crank-Nicolson type.

$$\frac{U_{i,j-1}^{n+1} - U_{i-1,j-1}^{n+1} + U_{i,j}^{n+1} - U_{i-1,j}^{n+1} + U_{i,j-1}^n - U_{i-1,j-1}^n + U_{i,j}^n - U_{i-1,j}^n}{4\Delta X} + \frac{V_{i,j}^{n+1} - V_{i,j+1}^{n+1} + V_{i,j}^n - V_{i,j-1}^n}{2\Delta Y} = 0 \quad (14)$$

$$\frac{U_{i,j}^{n+1} - U_{i,j}^n}{\Delta t} + U_{i,j}^n \frac{(U_{i,j}^{n+1} - U_{i-1,j}^{n+1} + U_{i,j}^n - U_{i-1,j}^n)}{2\Delta X} + V_{i,j}^n \frac{(U_{i,j+1}^{n+1} - U_{i,j-1}^{n+1} + U_{i,j+1}^n - U_{i,j-1}^n)}{4\Delta Y} = Gr^{1/4} \cos\phi \frac{\partial}{\partial X} \int T dY \quad (15)$$

$$\begin{aligned} & + \sin\phi \frac{[T_{i,j}^{n+1} + T_{i,j}^n]}{2} + \frac{(U_{i,j-1}^{n+1} - 2U_{i,j}^{n+1} + U_{i,j+1}^{n+1} + U_{i,j-1}^n - 2U_{i,j}^n + U_{i,j+1}^n)}{2(\Delta Y)^2} \\ & \frac{T_{i,j}^{n+1} - T_{i,j}^n}{\Delta t} + U_{i,j}^n \frac{(T_{i,j}^{n+1} - T_{i-1,j}^{n+1} + T_{i,j}^n - T_{i-1,j}^n)}{2\Delta X} \\ & + V_{i,j}^n \frac{(T_{i,j+1}^{n+1} - T_{i,j-1}^{n+1} + T_{i,j+1}^n - T_{i,j-1}^n)}{4\Delta Y} \\ & = \frac{1}{Pr} \frac{(T_{i,j-1}^{n+1} - 2T_{i,j}^{n+1} + T_{i,j+1}^{n+1} + T_{i,j-1}^n - 2T_{i,j}^n + T_{i,j+1}^n)}{2(\Delta Y)^2} \end{aligned} \quad (16)$$

Now, we consider the solution of the two-dimensional equation using the Crank-Nicolson method. The finite difference grid advances the solution from the time level (n) to the time level (n+1) as illustrated in Fig. 2. For the Dirchilet boundary conditions (i.e., the value of the function is specified at the boundaries), the finite difference equations must be applied at the interior points.

The region of integration is considered as a rectangle with sides X_{max} (=1) and Y_{max} (=14), where Y_{max} corresponds to $Y = \infty$, which lies very well outside the momentum and energy boundary layers. The maximum of Y was chosen as 14 after some preliminary investigations so that the last two of the boundary conditions (9) are satisfied. Here, the subscript i- designates the grid point along the X-direction, the j- along the Y direction, and the superscript n along the t direction. At any one time step, the coefficients $U_{i,j}^n$ and $V_{i,j}^n$ appearing in the difference equations are treated as constants. The values of U, V, and T are known at all grid points at $t = 0$ from the initial conditions.

The computations of U, V, and T at the time level (n+1) using the values at the previous time level (n) are carried out as follows:

The finite difference Eq. (16) at every internal nodal point on a particular i-level constitutes a tridiagonal system of equations. Such systems of equations are solved using the Thomas algorithm as de-

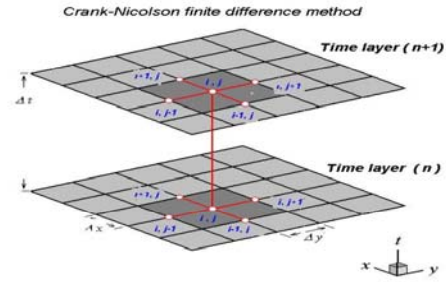


Fig. 2. The grid system.

scribed in the work of Carnahan et al. [19]. Thus, the values of T are found at every nodal point for a particular i at the (n+1)th time level. Using the values of T at the (n+1)th time level in Eq. (15), the values of U at the (n+1)th time level are found in a similar manner. Thus, the values of T and U are known on a particular i-level. Finally, the values of V are calculated explicitly using Eq. (14) at every nodal point on a particular i-level at the (n+1)th time level. This process is repeated for various i-levels. Thus, the values of T, U, and V are known at all grid points in the rectangular region at the (n+1)th time level.

Computations are carried out until the steady state is reached. The steady-state solution is assumed to have been reached when the absolute difference between the values of U, as well as temperature T, at two consecutive time steps is less than 10^{-5} at all grid points. After experimenting with a few sets of mesh sizes, they have been fixed at the level $\Delta X=0.05$, $\Delta Y=0.25$, and the time step $\Delta t=0.01$. In this case, the spatial mesh sizes are reduced by 50% in one direction, then in both directions; the results are compared. It is observed that when the mesh size is reduced by 50% in the X and Y directions, the results differ in the fourth decimal place. Hence, the above-mentioned sizes have been considered as the appropriate mesh sizes for calculation.

The derivatives involved in Eqs. (10)-(13) are evaluated using a five-point approximation formula, and then the integrals are evaluated using the Newton-Cotes closed integration formula.

4. Stability of the scheme

The stability criterion of the finite difference scheme for constant mesh sizes is examined using the Von-Neumann technique as explained by Carnahan et al. [19]. The general term of the Fourier expansion for U and T at a time arbitrarily called $t=0$ is assumed to

be of the form $e^{i\alpha X} e^{i\beta Y}$ (here $i = \sqrt{-1}$). At a later time t , these terms will become

$$\begin{aligned} U &= F(t)e^{i\alpha X} e^{i\beta Y} \\ T &= G(t)e^{i\alpha X} e^{i\beta Y} \end{aligned} \tag{17}$$

Then we substitute Eq. (17) in Eqs. (15) and (16) under the assumption that the coefficients U and T are constants over any one time step and denoting the values after one time step by F' and G' . After simplification, we obtain

$$\begin{aligned} \frac{(F' - F)}{\Delta t} + \frac{U}{2} \frac{(F' + F)(1 - e^{-i\alpha\Delta X})}{\Delta X} + \frac{V}{2} \frac{(F' + F)i \sin \beta\Delta Y}{\Delta Y} \\ = Gr^{-1/4} (\cos \phi) \frac{\alpha}{\beta} G(e^{i\beta Y_\infty} - e^{i\beta Y}) e^{-i\beta Y} + \frac{(G' + G)}{2} (\sin \phi) \\ + \frac{(F' + F)(\cos \beta\Delta Y - 1)}{(\Delta Y)^2} \end{aligned} \tag{18}$$

$$\begin{aligned} \frac{(G' - G)}{\Delta t} + \frac{U}{2} \frac{(G' + G)(1 - e^{-i\alpha\Delta X})}{\Delta X} \\ + \frac{V}{2} \frac{(G' + G)i \sin \beta\Delta Y}{\Delta Y} \\ = \frac{1}{Pr} \frac{(G' + G)(\cos \beta\Delta Y - 1)}{(\Delta Y)^2} \end{aligned} \tag{19}$$

Eqs. (18) and (19) can be rewritten as

$$\begin{aligned} (1 + A)F' &= (1 - A)F \\ &+ [Gr^{-1/4} (\cos \phi) \frac{\alpha}{\beta} G(e^{i\beta Y_\infty} - e^{i\beta Y}) e^{-i\beta Y} \\ &+ \frac{(G' + G)}{2} (\sin \phi)] \Delta t \end{aligned} \tag{20}$$

$$(1 + B)G' = (1 - B)G \tag{21}$$

where

$$\begin{aligned} A &= \frac{U}{2} \frac{\Delta t}{\Delta X} (1 - e^{-i\alpha\Delta X}) \\ &+ \frac{V}{2} \frac{\Delta t}{\Delta Y} i \sin(\beta\Delta Y) - (\cos \beta\Delta Y - 1) \frac{\Delta t}{(\Delta Y)^2} \\ B &= \frac{U}{2} \frac{\Delta t}{\Delta X} (1 - e^{-i\alpha\Delta X}) + \frac{V}{2} \frac{\Delta t}{\Delta Y} i \sin(\beta\Delta Y) \\ &- \frac{(\cos \beta\Delta Y - 1)}{Pr} \frac{\Delta t}{(\Delta Y)^2} \end{aligned}$$

After eliminating G' in Eq. (20) using Eq. (21), the resultant equation is given by

$$\begin{aligned} (1 + A)F' &= (1 - A)F + G[Gr^{-1/4} (\cos \phi) \frac{\alpha}{\beta} (e^{i\beta Y_\infty} - e^{i\beta Y}) e^{-i\beta Y} \\ &+ \frac{(\sin \phi)}{(1 + B)}] \Delta t \end{aligned} \tag{22}$$

Eqs. (22) and (21) can be written in matrix form:

$$\begin{bmatrix} F' \\ G' \end{bmatrix} = \begin{bmatrix} \frac{1-A}{1+A} & D_1 \\ 0 & \frac{1-B}{1+B} \end{bmatrix} \begin{bmatrix} F \\ G \end{bmatrix} \tag{23}$$

where

$$\begin{aligned} D_1 &= \frac{\Delta t}{(1+A)} [Gr^{-1/4} (\cos \phi) \frac{\alpha}{\beta} (e^{i\beta Y_\infty} - e^{i\beta Y}) e^{-i\beta Y} \\ &+ \frac{(\sin \phi)}{(1+B)}] \end{aligned}$$

Now, for the stability of the finite difference scheme, the modulus of each eigen value of the amplification matrix does not exceed unity. Since matrix Eq. (23) is triangular, the eigen values are its diagonal elements. The eigen values of the amplification matrix are $(1-A)/(1+A)$ and $(1-B)/(1+B)$. Assuming that U is everywhere non-negative, and V is everywhere non-positive, we obtain

$$\begin{aligned} A &= 2a \sin^2 \left(\frac{\alpha\Delta X}{2} \right) + 2c \sin^2 \left(\frac{\beta\Delta Y}{2} \right) \\ &+ i(a \sin(\alpha\Delta X) - b \sin(\beta\Delta Y)) \end{aligned}$$

where

$$a = \frac{U}{2} \frac{\Delta t}{\Delta X}, \quad b = \frac{|V|}{2} \frac{\Delta t}{\Delta Y}, \quad c = \frac{\Delta t}{(\Delta Y)^2}$$

Because the real part of A is greater than or equal to zero, $|(1-A)/(1+A)| \leq 1$ always. Similarly, $|(1-B)/(1+B)| \leq 1$.

Hence, the finite difference scheme is unconditionally stable. The local truncation error is $O(\Delta t^2 + \Delta Y^2 + \Delta X)$, and it tends to be zero as Δt , ΔX , and ΔY also tend to be zero. Hence, the scheme is compatible. Stability and compatibility ensure convergence.

5. Results and discussion

To assess the accuracy of the numerical results, the present result is compared with previous studies available in the literature. The velocity profiles for $\phi = 57.65^\circ$, $Gr = 10^6$, and $Pr = 0.7$ are compared with the theoretical results of the work of Chen et al. [3] as shown in Fig. 3, which are found to be in good agreement.

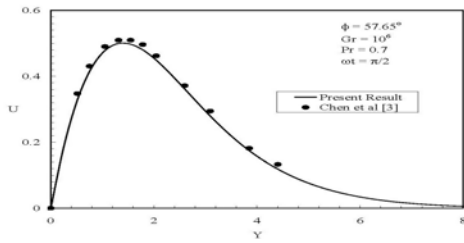


Fig. 3. Comparison of velocity profiles at X=1.0

The transient velocity profiles at X=1.0 for different values of the Grashof number and the inclination angle ϕ to the horizontal are presented in Fig. 4. Velocity increases steadily as time advances, and it reaches a temporal maximum and consequently the steady state because the tangential component of the buoyancy force increases with ϕ and dominates in the downstream. A higher velocity is experienced throughout the transient period as well as in the steady-state level for a system having larger angles of inclination to the horizontal. The difference between the temporal maximum and the steady state decreases as ϕ increases. The velocity of air decreases as Gr increases.

In Fig.5, the transient velocity profiles are plotted for different values of the Prandtl number of the fluid Pr and the frequency parameter ωt . It is observed that there is a decrease in the velocity of the fluid when Pr increases (i.e., for Pr=0.71 (air), 7.0 (water)). The higher the values of Pr, the higher is the rate of heat transfer; hence, the time taken to reach the steady state is high for higher values of Pr. The difference between the temporal maximum and steady state decreases with an increase in the value of the Prandtl number of the fluid. For the frequency parameter ωt , the velocity is observed to decrease for an increase in the value of ωt . The time taken to reach the steady state increases as ωt increases. It is also observed that the temporal maximum for velocity increases with an increase in the value of ωt .

The profiles of transient temperature for various values of the Grashof number and the inclination angle ϕ are shown in Fig. 6. The temperature profiles presented are those at the leading edge of the plate, that is, at X=1.0. We observe from this figure that a lower temperature is experienced for a system having a higher value of ϕ . The effect of Grashof number on the temperature profile is nil.

The effects of Prandtl number Pr and the frequency parameter ωt on temperature are shown in Fig. 7. The

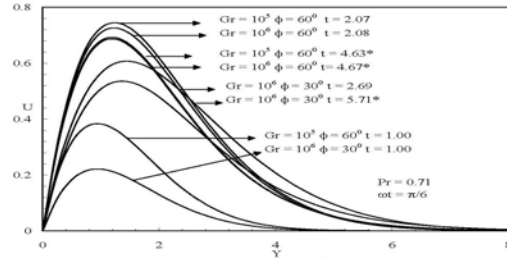


Fig. 4. Transient velocity profiles at X=1.0 for different Gr and ϕ (*-steady state).

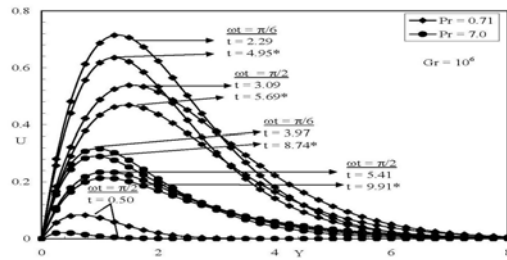


Fig. 5. Transient Velocity profiles at X=1.0 for different Pr and ωt (*-steady state).

larger value of Pr gives rise to the thinner thermal boundary layer because increasing the value of Pr gives rise to a higher heat transfer. The temporal maximum is attained at an early stage for lower values of the frequency parameter ωt . It is also observed that the temperature profiles decrease with an increase in the value of ωt .

In Fig. 8, the values of local shear stress are plotted for various values of Pr, ϕ , and ωt . The local wall shear stress decreases as ϕ decreases because the velocity decreases with a decrease in the value of ϕ as shown in Fig. 4. The increasing value of Pr gives rise to a lower shear stress, which is also observed in Fig. 5. This is quite expected because increasing Pr gives a thicker velocity profile, which in turn results in a lower shear stress value. It is also observed that shear stress decreases as ωt increases.

The steady-state local Nusselt number, that is, the local heat transfer rate, is plotted in Fig. 9. It increases as X increases. The local heat transfer is stronger on Pr than on the other parameters because a lower Pr results in thicker temperature profiles. It is also observed that the local Nusselt number increases with an increase in the value of ϕ . But local Nusselt number decreases as ωt increases.

The average values of skin friction and the Nusselt number are shown in Figs. 10 and 11, respectively. In

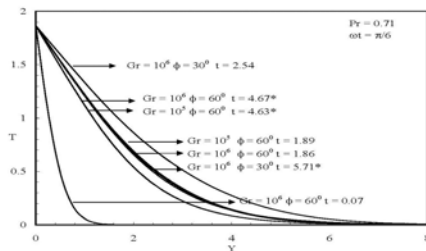


Fig. 6. Transient temperature profiles at X=1.0 for different Gr and ϕ (*-steady state).

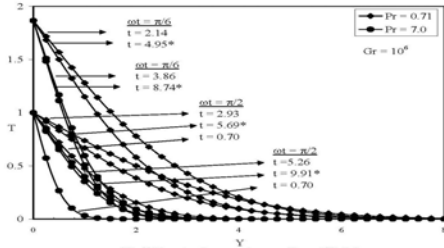


Fig. 7. Transient temperature profiles at X=1.0 for different Pr and ωt (*-steady state).

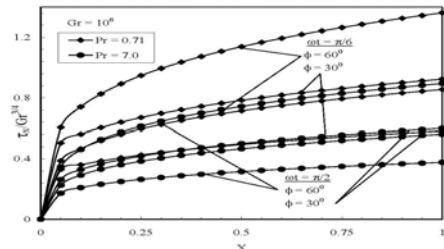


Fig. 8. Local skin friction.

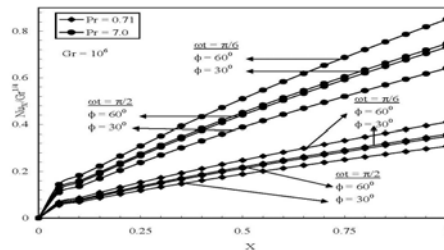


Fig. 9. Local Nusselt number.

Fig. 10, it is observed that the average skin friction increases with time and reaches the steady state after some time. Owing to inclination with the horizontal, the average skin friction is found to decrease. A lower value of skin friction is observed for a higher value of Pr and ωt .

The average Nusselt number is the same at a particular time level in the initial period for a fixed Pr. This shows that there is only heat conduction in the initial time level. The average Nusselt number de-

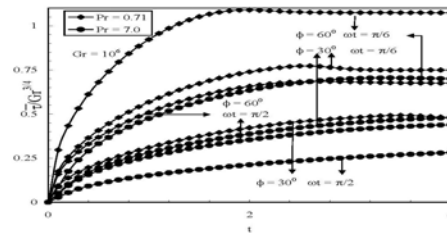


Fig. 10. Average skin friction.

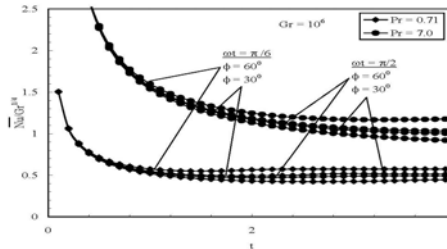


Fig. 11. Average Nusselt number.

creases as ϕ decreases. Furthermore, it is noticed that the average Nusselt number decreases with an increase in the value of ωt .

6. Conclusion

Unsteady natural convection flow past a semi-infinite inclined plate with oscillating temperature is considered in this paper. The governing partial differential equations are transformed into a set of dimensionless governing equations, which are solved numerically by using an implicit finite difference method. The conclusions of the study are as follows:

- (1) The difference between the temporal maximum and the steady-state value is reduced when ϕ increases.
- (2) The velocity is observed to be maximum near the upstream and decreases in the flow direction.
- (3) Velocity and temperature are found to decrease when the frequency parameter ωt increases.
- (4) The local shear stress decreases as ωt increases.
- (5) The local Nusselt number increases with an increase in the value of the inclination angle ϕ .

Acknowledgment

This work was supported by the BK21 Research Program, Inha University, Korea.

References

[1] T. Fujii and H. Imura, Natural Convection heat

- transfer from a plate with arbitrary inclination, *Int. J. Heat Mass Tr.* 15 (1972) 1873-1886.
- [2] L. Pera and B. Gebhart Natural Convection boundary layer flow over horizontal and slightly inclined surfaces, *Int. J. Heat Mass Tr.* 16 (1973) 1131-1146.
- [3] T. S. Chen H. C. Tien and B. F. Armaly, Natural Convection on horizontal, inclined and vertical plates with variable surface temperature or heat flux, *Int. J. Heat Mass Transfer.* 29 (1986) 1465-1478.
- [4] K. Ekambavannan and P. Ganesan, Finite difference solution of unsteady natural convection boundary layer flow over an inclined plate with variable surface temperature, *Wärme and Stoffübertragung*, 30 (1994), 63-69.
- [5] M. D. Kelleher and K. T. Yang, Heat transfer responses of laminar free convection boundary layers along a vertical heated plate to surface temperature oscillations, *J. Appl. Math. Phys.* 19 (1968) 31-44.
- [6] V. M. Soundalgekar and M. R., Patil, Stoke's problem for a vertical infinite plate with variable temperature, *Astrophysics and Space Sci.* 59 (1978) 503-506.
- [7] V. M. Soundalgekar, Free convection effects on the flow past an infinite vertical oscillating plate, *Astrophysics and Space Sci.* 64 (1979) 165-171.
- [8] V. M. Soundalgekar, Unsteady forced and free convective flow past an infinite vertical porous plate with oscillating wall temperature and constant suction, *Astrophysics and Space Sci.* 66 (1979) 223-233.
- [9] R. L. Verma, Free convection fluctuating boundary layer on a horizontal plate, *J. Appl. Math. Mech.* 63 (1982) 483-487.
- [10] V. M. Soundalgekar, N. S. Birajdar and V. K. Darwhekar, Mass-Transfer effects on the flow past an impulsively started infinite vertical plate with variable temperature or constant heat flux, *Astrophysics and Space Sci.* 100 (1984) 159-164.
- [11] M. A. Hossain, Simultaneous heat and mass transfer on oscillatory free convection boundary layer flow, *Int. J. Energy Research*, 12 (1998) 205-206.
- [12] U. N. Das R. K. Deka and V. M. Soundalgekar, Transient free convection flow past an infinite vertical plate with periodic temperature variation, *Trans. ASME, J. Heat Tr.* 121 (1999) 2629-2632.
- [13] M. A. Hossain, S. K. Das and I. Pop, Heat transfer response of MHD free convection along a vertical plate to surface temperature oscillations, *Int. J. Non-linear Mechanics.* 33 (1998) 541-553.
- [14] Shripad T. Revankar, Free convection effect on a flow past an impulsively started or oscillating infinite vertical plate, *Mechanics Research Communications.* 27 (2) (2000) 241-246.
- [15] J. Li, D. Ingham and I. Pop, Natural convection from a vertical plate with a surface temperature oscillation, *Int. J. Heat Mass Tr.* 44 (2001) 2311-2322.
- [16] T. Lorenzo and J. Padet, Parametric study of transient free convection heat transfer, *Int. J. Heat Mass Tr.* 45 (2002) 2629-2632.
- [17] H. P. Rani and R. Devaraj, Numerical solution of unsteady flow past a vertical cylinder with temperature oscillations, *Forschung im Ingenieurwesen.* 68 (2003) 75-78.
- [18] Nawaf H. Saeid., Periodic free convection from vertical plate subjected to periodic surface temperature oscillating, *Int. J. thermal sci.* 43 (2004) 569-574.
- [19] B. Carnahan, H. A. Luther and J. O. Wilkes, Applied Numerical Methods. *John Wiley and Sons*, 1969.



G. Palani received his B.Sc. and M.Sc. degrees from Madras University, India, in 1991 and 1993, respectively, and his Ph.D. degree from Anna University, India in 2001. Dr. G. Palani is currently a Post Doctoral Engineering Fellow at the School of Mechanical Engineering of Inha University in Incheon, Korea.



Kwang-Yong Kim received his B.S. degree from Seoul National University in 1978, and his M.S. and Ph.D. degrees from the Korea Advanced Institute of Science and Technology (KAIST), Korea, in 1981 and 1987, respectively. He is currently a professor and the chairman of the School of Mechanical Engineering of Inha University, Incheon, Korea. Professor Kim is also the current editor-in-chief of the Transactions of Korean Society of Mechanical Engineers (KSME), the editor-in-chief of the International Journal of Fluid Machinery and Systems (IJFMS), and the chief vice president of the Korean Fluid Machinery Association (KFMA). He is likewise a fellow of the American Society of Mechanical Engineers (ASME).